P. M.) 345–374 (Raven, New York, 1996).
11. Ahmed, R. *et al.* Selection of genetic variants of lymphocytic choriomeningitis virus in spleens of persistently infected mice: role in suppression of cytotoxic T lymphocyte response and viral persistence. *J. Exp. Med.* **160,** 521–540 (1984).
12. Byrne, J. A. & Oldstone, M. B. A. Biology of cloned cytotoxic T lymphocytes specific for lymphocytic choriomeningitis virus: clearance of virus in vivo. *J. Virol.* **51,** 682–686 (1984).
13. Moskophidis, D., Cobbold, S. P., Waldmann, H. & Lehmann-Grube, F. Mechanism of recovery from acute virus infection: treatment of lymphocytic choriomeningitis virus-infected mice with monoclonal antibodies reveals that Lyt-2$^+$ T lymphocytes mediate clearance of virus and regulate the antiviral antibody response. *J. Virol.* **61,** 1867–1874 (1987).
14. Whitton, J. L. Lymphocytic choriomeningitis virus CTL. *Semin. Virol.* **1,** 257–262 (1990).
15. Schulz, M. *et al.* Major histocompatibility complex-dependent T cell epitopes of lymphocytic choriomeningitis virus nucleoprotein and their protective capacity against viral disease. *Eur. J. Immunol.* **19,** 1657–1668 (1998).
16. Butz, E. A. & Bevan, M. J. Massive expansion of antigen-specific CD8$^+$ T cells during an acute virus infection. *Immunity* **8,** 167–175 (1998).
17. Murali-Krishna, K. *et al.* Counting antigen-specific CD8 T cells: a reevaluation of bystander activation during viral infection. *Immunity* **8,** 177–187 (1998).
18. Whitton, J. L. *et al.* Molecular analyses of a five-amino-acid cytotoxic T-lymphocyte (CTL) epitope: an immunodominant region which induces nonreciprocal CTL cross-reactivity. *J. Virol.* **63,** 4303–4310 (1989).
19. Yang, Y., Chang, J. F., Parnes, J. R. & Fathman, C. G. T cell receptor (TCR) engagement leads to activation-induced splicing of tumor necrosis factor (TNF) nuclear pre-mRNA. *J. Exp. Med.* **188,** 247–254 (1998).
20. Flynn, K. J. *et al.* Virus-specific CD8$^+$ T cells in primary and secondary influenza pneumonia. *Immunity* **8,** 683–691 (1998).
21. Sachs, A. B. Messenger RNA degradation in eukaryotes. *Cell* **74,** 413–421 (1993).
22. Hayden, F. G. *et al.* Local and systemic cytokine responses during experimental human influenza A virus infection. Relation to symptom formation and host defense. *J. Clin. Invest.* **101,** 643–649 (1998).
23. Campbell, I. L. Neuropathogenic actions of cytokines assessed in transgenic mice. *Int. J. Dev. Neurosci.* **13,** 275–284 (1995).
24. Masuda, N. *et al.* Interleukin 6 is a cause of flu-like symptoms in treatment with a deoxycytidine analogue. *Br. J. Cancer* **78,** 388–389 (1998).
25. Selin, L. K., Varga, S. M., Wong, I. C. & Welsh, R. M. Protective heterologous antiviral immunity and enhanced immunopathogenesis mediated by memory T cell populations. *J. Exp. Med.* **188,** 1705–1715 (1998).
26. Tracey, K. J. & Cerami, A. Tumor necrosis factor and regulation of metabolism in infection: role of systemic versus tissue levels. *Proc. Soc. Exp. Biol. Med.* **200,** 233–239 (1992).

Supplementary information is available on *Nature*'s World-Wide Web site (http://www.nature.com) or as paper copy from the London editorial office of *Nature*.

Acknowledgements

We thank A. Lord for administrative assistance. The work was supported by grants from the NIH (J.L.W. and M.K.S.) and by Eusko Juarlaritza (F.R.).

Correspondence and requests for materials should be addressed to M.K.S. (e-mail: mslifka@scripps.edu).

Cell transformation by the superoxide-generating oxidase Mox1

Young-Ah Suh*‡, Rebecca S. Arnold*‡, Bernard Lassegue†, Jing Shi*, Xiangxi Xu*, Dan Sorescu†, Andrew B. Chung†, Kathy K. Griendling† & J. David Lambeth*

*Departments of * Biochemistry and † Medicine, Emory University Medical School, Atlanta, Georgia 30322, USA*
‡ These authors contributed equally to this work.

Reactive oxygen species (ROS) generated in some non-phagocytic cells are implicated in mitogenic signalling and cancer[1–6]. Many cancer cells show increased production of ROS[7], and normal cells exposed to hydrogen peroxide or superoxide show increased proliferation[8] and express growth-related genes[9–11]. ROS are generated in response to growth factors, and may affect cell growth[2,3,12,13], for example in vascular smooth-muscle cells[6,13–15]. Increased ROS in *Ras*-transformed fibroblasts correlates with increased mitogenic rate[16]. Here we describe the cloning of *mox1*, which encodes a homologue of the catalytic subunit of the superoxide-generating NADPH oxidase of phagocytes[17,18], gp91*phox*. *mox1* messenger RNA is expressed in colon, prostate, uterus and vascular smooth muscle, but not in peripheral blood leukocytes. In smooth-muscle cells, platelet-derived growth factor induces *mox1* mRNA production, while antisense *mox1* mRNA decreases superoxide generation and serum-stimulated growth. Overexpression of *mox1* in NIH3T3 cells increases superoxide generation and cell growth. Cells expressing *mox1* have a transformed appearance, show anchorage-independent growth and produce tumours in athymic mice. These data link ROS production by Mox1 to growth control in non-phagocytic cells.

A human expressed sequence tag (EST) sequence which showed homology to human gp91*phox* was identified, and complete sequencing revealed a predicted amino-acid sequence homologous to the carboxy-terminal half of gp91*phox*. Sequencing was completed with 5′-rapid amplification of complementary DNA ends (5′-RACE) using human colon cDNA, and the predicted amino-acid sequence is shown in Fig. 1. The predicted protein is 564 amino acids long, compared with 569 residues for gp91*phox*, and the two show 56% identity. The gene is located at Xq22 (Genebank accession no. Z83819), but the locus is not informative with regard to known diseases. Rat *mox1*, cloned by using degenerate primers based on sequences that are highly conserved between gp91*phox* and human *mox1*, is 82% identical to human *mox1* (Fig. 1). Human and rat Mox1 lack asparagine-linked candidate glycosylation sites, which are seen in the highly glycosylated human and mouse

```
                1                                   †      50
gp91phox/human  MGNWAVNEGLSIFAILVWLGLNVFLFVWYYRVYDIPPKFFYTRKLLGSAL
  p65mox/human  MGNWVVNHWFSVLFLVVWLGLNVFLFVDAFLKYEKADKYYYTRKILGSTL
    p65mox/rat  MGNWLVNHWLSVLFLVSWLGLNIFLFVYVFLNYEKSDKYYYTREILGTAL

               51                                          100
gp91phox/human  ALARAPAACLNFNCMLILLPVCRNLLSFLRGSSACCSTRVRRQLDRNLTF
  p65mox/human  ACARASALCLNFNSTLILLPVCRNLLSFLRGTCSFCSRTLRKQLDHNLTF
    p65mox/rat  ALARASALCLNFNSMVILIPVCRNLLSFLRGTCSFCNHTLRKPLDHNLTF

               ●          ● ●          ‡                   148
gp91phox/human  HKMVAWMIALHSAIHTIAHLFNVEWCVNARVNNSDPYSVALSEL..GDRQ
  p65mox/human  HKLVAYMICLHTAIHIIAHLFNFDCYSRSRQATDGSLASILSSLSHDEKK
    p65mox/rat  HKLVAYMICIFTAIHIIAHLFNFERYSRSQQAMDGSLASVLSSLFHPEKE

               ‡                                           197
gp91phox/human  NESYLNFARKRIKNPEGGL.YLAVTLLAGITGVVITLCLILIIITSSTKTI
  p65mox/human  GGSWLN....PIQSRNTTVEYVTFTSVAGLTGVIMTIALILMVTSATEFI
    p65mox/rat  D.SWLN....PIQSPNVTVMYAAFTSIAGLTGVVATVALVLMVTSAMEFI

               198        ●●          ●              ‡      247
gp91phox/human  RRSYFEVFWYTHHLFVIFFIGLAIHGAERIVRGQTAESLAVHNITVCEQK
  p65mox/human  RRSYFEVFWYTHHLFIFYILGLGIHGIGGIVRGQTEESMNESHPRKCAES
    p65mox/rat  RRNYFELFWYTHHLFIIYIICLGIHGLGGIVRGQTEESMSESHPRNCSYS

               248                                         296
gp91phox/human  ISEWGKIK.ECPIPQFAGNPPMTWKWIVGPMFLYLCERLVRFWRSQQKVV
  p65mox/human  FEMWDDRDSHCRRPKFEGHPPESWKWILAPVILYICERILRFYRSQQKVV
    p65mox/rat  FHEWDKYERSCRSPHFVGQPPESWKWILAPIAFYIFERILRFYRSRQKVV

               297                                         346
gp91phox/human  ITKVVTHPFKTIELQMKKKGFKMEVGQYIFVKCPKVSKLEWHPFTLTSAP
  p65mox/human  ITKVVMHPSKVLELQMNKRGFSMEVGQYIFVNCPSISLLEWHPFTLTSAP
    p65mox/rat  ITKVVMHPCKVLELQMRKRGFTMGIGQYIFVNCPSISFLEWHPFTLTSAP
                                                  1a
               347                                         395
gp91phox/human  EEDFFSIHIRIVGDWTEGLFNACGCDKQEFQDAWK.LPKIAVDGPFGTAS
  p65mox/human  EEDFFSIHIRAAGDWTENLIRA.......FEQQYSPIPRIEVDGPFGTAS
    p65mox/rat  EEEFFSIHIRAAGDWTENLIRT.......FEQQHSPMPRIEVDGPFGTVS
                   1b
               396                                         445
gp91phox/human  EDVFSYEVVMLVGAGIGVTPFASILKSVWYKYCNNATNLKLKKIYFYWLC
  p65mox/human  EDVFQYEVAVLVGAGIGVTPFASILKSIWYKFQCADHNLKTKKIYFYWIC
    p65mox/rat  EDVFQYEVAVLVGAGIGVTPFASFLKSIWYKFQRAHNKLKTQKIYFYWIC
                          2a                                2b
               446                                         495
gp91phox/human  RDTHAFEWFADLLQLLESQMQERNNAGFLSYNIYLTGWDESQANHFAVHH
  p65mox/human  RETGAFSWFNNLLTSLEQEMEELGKVGFLNYRLFLTGWDSNIVGHAALNF
    p65mox/rat  RETGAFAWFNNLLNSLEQEMDELGKPDFLNYRLFLTGWDSNIAGHAALNF

               496                                         545
gp91phox/human  DEEKDVITGLKQKTLYGRPNWDNEFKTIASQHPNTRIGVFLCGPEALAET
  p65mox/human  DKATDIVTGLKQKTSFGRPMWDNEFSTIATSHPKSVVGVFLCGPRTLAKS
    p65mox/rat  DRATDVLTGLKQKTSFGRPMWDNEFSRIATAHPKSVVGVFLCGPPTLAKS
                          2c                                2d
               546
gp91phox/human  LSKQSISNSESGPRGVHFIFNKENF
  p65mox/human  LRKCCHRYSSLDPRKVQFYFNKENF
    p65mox/rat  LRKCCRRYSSLDPRKVQFYFNKETF
```

Figure 1 Predicted amino-acid sequence of human Mox1 (GenBank accession no. AF127763, patent pending) and rat Mox1 (GenBank accession no. AF152963), with human gp91*phox*. Abbreviations of amino-acid residues are according to standard IUPAC nomenclature. † and ‡ indicate asparagine-linked candidate glycosylation sites in mouse and human gp91*phox*, respectively. Filled circles indicate conserved histidines that are candidates for haem ligation.

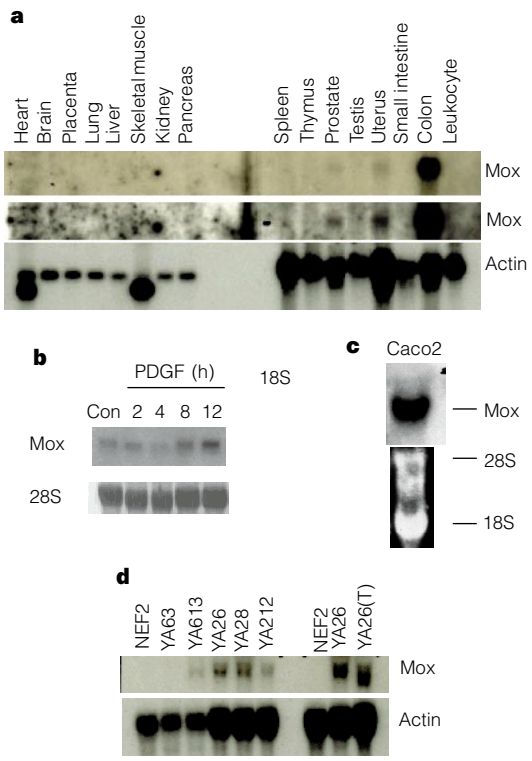

Figure 2 Expression of *mox1* mRNA. **a**, Tissue expression of human *mox1* mRNA. Top and middle panels were exposed for 24 h and 3 days, respectively. The bottom panel was probed for actin mRNA. **b**, Expression of rat-*mox1* mRNA in rat aortic smooth muscle and induction by 20 ng ml^{-1} PDGF. Bottom, 28S rRNA. **c**, Expression of human *mox1* in Caco-2 cells. **d**, Northern analysis of human-*mox1* mRNA in NIH 3T3 cells transfected with vector alone (NEF2) or with human-*mox1* (YA63, YA613, YA26, YA28 and YA212), and a tumour YA26(T) produced in athymic mice after injection of *mox1*-expressing cells.

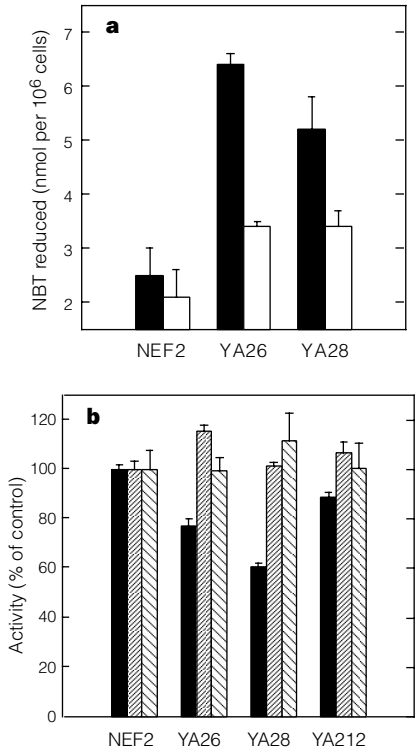

Figure 3 Superoxide generation by Mox1. **a**, Reduction of nitroblue tetrazolium (NBT) in *mox1*-transfected and control fibroblasts was measured in the absence (filled bars) or presence (open bars) of superoxide dismutase. **b**, Aconitase (filled bars), lactate dehydrogenase (narrow hatching) and fumarase (broad hatching) were determined in lysates of cells transfected with vector alone (NEF2) or with *mox1* (YA26, YA28 and YA212). Results are the average ± s.e.m. of 3 experiments. Activities are expressed as percentage of that seen in NEF2 cells.

gp91*phox*[19,21] (the positions of which are indicated by ‡ and †, respectively, in Fig. 1). Regions in gp91*phox* (underlined), which were previously proposed[21–22] to be binding sites for flavin (regions 1a and 1b) and pyridine nucleotide (regions 2a–2d), are identical or nearly identical between gp91*phox* and Mox1. Also shown (filled circles) are conserved histidines, which are candidates for haem ligation. The hydropathy profiles of human gp91*phox* and Mox1 are nearly identical (not shown), and include five very hydrophobic stretches in the amino-terminal half of the molecules which are predicted to be membrane-spanning regions.

The distribution in the tissues of *mox1* mRNA was very different from that of gp91*phox*. Among normal human tissues, *mox1* was expressed most in colon, and low expression was also detected in the uterus and prostate (Fig. 2a). The human colon-carcinoma cell line Caco-2 also expressed large quantities of *mox1* message (Fig. 2c). In cultured rat aortic vascular smooth-muscle cells (Fig. 2b), platelet-derived growth factor (PDGF), which causes cell proliferation[13,24], induced a roughly twofold increase in the expression of rat *mox1* mRNA within 12 hours of treatment, consistent with the idea that Mox1 contributes to the growth-stimulatory effects of PDGF.

To investigate whether Mox1 catalysed superoxide generation in cells, *mox1* DNA was stably transfected into NIH 3T3 cells. After selection, 30 surviving colonies were screened by the polymerase chain reaction with reverse transcription (RT-PCR) for expression of *mox1* mRNA (not shown), and 22 of these showed expression of *mox1* message. Five colonies were selected for further analysis, of which four (YA613, YA26, YA28 and YA212) showed significant expression of *mox1* message (Fig. 2d). Superoxide generation by intact cells was monitored by using superoxide dismutase-sensitive reduction of nitroblue tetrazolium (Fig. 3a). YA26 and YA28 cells showed increased reduction of nitroblue tetrazolium compared with vector (NEF2)-transfected cells, much of which was inhibited by superoxide dismutase. Because superoxide dismutase and nitroblue tetrazolium are not likely to penetrate cells, superoxide must be generated extracellularly. The amount of superoxide generated by these cells is on the order of 0.3–0.6 nmol min^{-1} per 10^6 cells, or about 5–10% of that generated by activated human neutrophils. NADPH-dependent superoxide generation was measured in broken cell preparations by using a lucigenin luminescence assay. Although substantial background signal was seen, luminescence was about twofold higher in *mox1*-transfected cells than in vector-transfected cells, and was inhibited by both superoxide dismutase and the general flavoprotein inhibitor diphenylene iodonium (not shown). This signal was unaffected by added recombinant human p47*phox*, p67*phox* and Rac1(GTP-γS), which are essential cytosolic factors for the phagocyte respiratory-burst oxidase. Thus, *mox1*-transfected cells show increased superoxide generation compared with control cells.

To test whether superoxide generated by Mox1 can affect intracellular 'targets', we monitored aconitase activity in control and in three *mox1*-transfected cell lines. Aconitase contains a four-iron-four-sulphur cluster, which is highly susceptible to modification by superoxide, resulting in a loss in enzyme activity[25,26], and has been used as a reporter of intracellular superoxide generation. Aconitase activity was significantly diminished in YA26, YA28 and YA212 cells compared with the transfected control (Fig. 3b), and the decrease in activity paralleled the expression of *mox1* in these cells (compare with Fig. 2d). Approximately 50% of the aconitase in these cells is mitochondrial, based on differential centrifugation, and the cytosolic and mitochondrial forms were both affected (not shown).

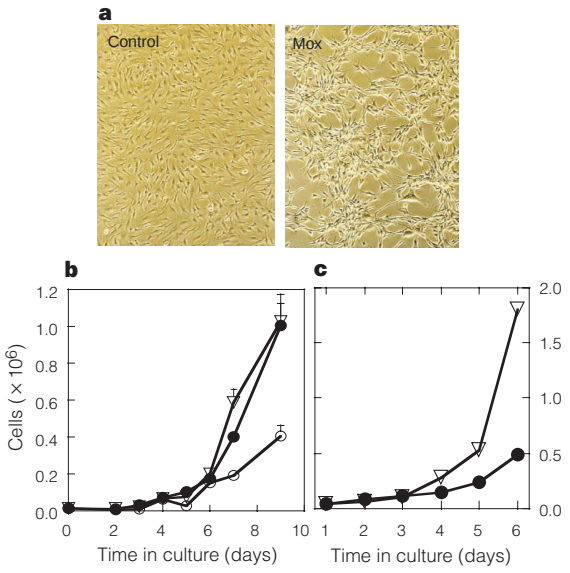

Figure 4 Properties of NIH 3T3 cells transfected with *mox1*. **a**, Control NIH 3T3 (left) and YA28 cells stably transfected with *mox1* (right) grown in culture for 3 days and observed by light microscopy (original magnification ×100). **b**, Growth curves for vector control (NEF2) cell line (open circles) and YA26 (filled circles) and YA28 (open triangles) *mox1*-transfected cell lines. Cells were plated at 13×10^4 cells per well in 6-well plates. Triplicates ± s.e.m. are shown. **c**, Growth curves for YA28 cells in the absence (open triangles) or presence (filled circles) of 20 mM N-acetyl cysteine added daily to cultures.

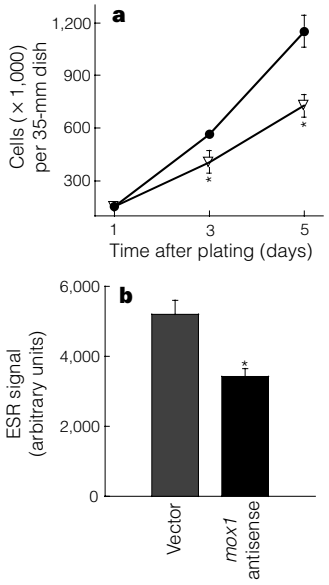

Figure 5 Role of Mox1 in growth of vascular smooth-muscle cells. **a**, Cells were transfected with antisense rat *mox1* (open triangles) or empty vector (filled circles), and cell number was quantified using a Coulter counter. Values are the mean ± s.e.m. of 3 experiments; $^*P < 0.001$. **b**, Cells were transfected with antisense rat *mox1* or empty vector and were analysed for superoxide by electrospin resonance (ESR). Bars show the mean ± s.e.m. of 3 independent experiments. $^*P = 0.03$.

Control cytosolic and mitochondrial enzymes that do not contain iron–sulphur centres were not affected (Fig. 3b). Superoxide generated in *mox1*-transfected cells is therefore capable of reacting with and modifying intracellular components.

Remarkably, *mox1*-transfected NIH 3T3 cells grown in culture take on a transformed appearance, becoming elongated and losing contact inhibition (Fig. 4a). Of 13 cell lines developed from *mox1*-transfected cells, 11 (85%) showed a transformed phenotype, whereas none of 22 lines (0%) isolated from cells transfected with vector alone showed this phenotype. The *mox1* cells retain a partial dependence on serum for growth (not shown), and growth rates in the presence of serum are increased (Fig. 4b). Growth of the *mox1*-transfected cells was inhibited by the antioxidant *N*-acetyl cysteine (Fig. 4c), consistent with reactive oxygen acting as mediator in the regulation of cell division. The *mox1*-transfected cells exhibited anchorage-independent growth in soft agar (not shown), although colonies were smaller than those seen for *Ras*-transformed fibroblasts.

The *mox1*-transfected cells also produced aggressive tumours in athymic mice (not shown), which at about 3–4 weeks were similar in size to those produced by *ras*-transformed NIH 3T3 cells. Of 15 mice injected with *mox1*-transfected NIH 3T3 cells, 14 showed large tumours within 17 days of injection, and tumours showed expression of *mox1* mRNA (Fig. 2d). Histologically, the tumours resembled fibrosarcomas and were similar to *ras*-induced tumours (not shown). Thus, *ras* and *mox1* were similarly potent in their ability to induce tumorigenicity of NIH3T3 cells in athymic mice.

A role in normal growth was demonstrated in rat aortic vascular smooth-muscle cells by using antisense to rat *mox1*. Transfection with the antisense DNA resulted in a decrease in both superoxide generation (Fig. 5b) and serum-dependent growth (Fig. 5a). Mox1 is therefore implicated in normal growth in this cell type.

Our results show that Mox1, a homologue of gp91*phox*, generates ROS in some non-phagocytic cells and may participate in normal mitogenic regulation in response to growth factors, such as PDGF, and in disregulated growth in hyperproliferative disorders such as cancer and atherosclerosis. □

Methods

Cloning.

A homologous 334-base portion of an expressed sequence tag (EST176696; GenBank accession no. AA305700) from a Caco-2 cell line was identified by using the human gp91*phox* amino-acid sequence as a query in a Blast search. The bacterial strain #129134 containing the EST sequence in the pBluescript SK-vector was purchased from ATCC (Rockville). EST176696 encoded 337 amino acids showing homology to the C-terminal 60% of human gp91*phox*, and contained a stop codon corresponding to the C terminus of gp91*phox*. 5′-RACE, carried out using a human colon cDNA library and Marathon cDNA Amplification Kit (ClonTech, Palo Alto) using a gene-specific primer, yielded a 1.1-kilobase (kb) fragment containing an ATG codon corresponding in position to the start site in gp91*phox*. Reamplification with DNA primers spanning the putative start and stop codons yielded a 1.7-kb fragment which was TA-cloned into the PCR2.1 vector (Invitrogen TA Cloning Kit, San Diego).

A 1.1-kb central fragment of rat *mox1* cDNA was obtained by RT-PCR of vascular smooth-muscle-cell RNA using primers designed to anneal to human *mox1* and human, mouse and pig gp91*phox*. The sequence was extended by 5′- and 3′-RACE, which yielded 850-base pair and 1.5-kb products, respectively. Full-length rat *mox1* cDNA (2.6 kb) was obtained by RT-PCR of the smooth-muscle-cell RNA by using primers designed to anneal to the terminal segments of the 5′- and 3′-RACE products.

Transfections.

pEF-PAC vector alone and vector containing the subcloned coding region for *mox1* were stably transfected (10 μg DNA) into 2×10^6 NIH 3T3 cells by using Fugene 6 (Boehringer Mannheim). Cells maintained in DMEM containing 10% calf serum were split after 2 days and selected with 1 μg ml^{-1} puromycin. Colonies surviving in selection media for 10–14 days were subcultured and characterized for expression of *mox1* mRNA. For antisense experiments, cells plated at low density were transfected using Superfect reagent (Qiagen) with either full-length antisense rat-*mox1* in the pcDNA3 vector (Invitrogen) or empty vector. Cells were replated at higher density, allowed to grow in medium with 10% calf serum, 400 μg ml^{-1} geneticin and 10 mM glutamine and passaged 3–4 times in selection medium. Transcription from the empty vector and the antisense construct were verified by RT-PCR by using vector-specific primers.

Northern blots.

Human multiple tissue northern blot I and blot IV membranes (ClonTech) were incubated at 68 °C in hybridization solution for 1 h and hybridized (68 °C, 3–4 h) with radiolabelled *mox1* coding region. Human or rat *mox1* coding region was labelled by random priming with [^{32}P]dCTP (10 μCi) using the Prime-It II kit (Stratagene, La Jolla). For analysis of *mox1* mRNA expression in cell lines, total RNA was prepared from 10^6 cells using the High Pure RNA Isolation Kit (Boehringer Mannheim) or RNeasy kit (Qiagen, Valencia, CA). Total RNA (10–20 μg) was separated on a 1% agarose formaldehyde minigel and transferred to a Nytran filter (Biorad, Hercules, CA) and immobilized by ultraviolet crosslinking.

Nitroblue tetrazolium (NBT) reduction assay.

Cells (500,000 per well in six-well plates) were plated. After 24 h, medium was removed and cells were washed with 1 ml Hanks solution (Sigma). Filtered 0.25% NBT (1 ml, Sigma) was added with or without 600 units of superoxide dismutase (Sigma) and cells were incubated at 37 °C for 8 min. Cells were scraped and NBT was pelleted by low-speed centrifugation. The NBT pellet was resuspended in 1 ml of pyridine (Sigma) and solubilized by heating for 10 min at 100 °C. Reduced NBT was quantified by measuring the absorbance at 510 nm (extinction coefficient of 11,000 M^{-1} cm^{-1}).

Aconitase, lactate dehydrogenase and fumarase assays.

Aconitase, lactate dehydrogenase and fumarase activities were determined as described[25,27,28].

Superoxide measurement by spin trapping.

Transfected cells were washed twice with phosphate-buffered saline (PBS), sedimented at 400*g* for 10 min, resuspended and homogenized by sonication in 1 ml lysis buffer (50 mM Tris, 0.1 mM EDTA, 0.1 mM EGTA, aprotinin, leupeptin, pepstatin and PMSF). Membrane pellet (10 μg 28,000*g*) (resuspended in lysis buffer) was incubated with 10 mM DEPMPO (5-diethoxyphosphoryl-5-1-pyrroline-N-oxide, Oxis), 100 μM diethyldithiocarbamate, 100 μM NADPH, 0.1 mM diethylenetriaminepentaacetic acid in PBS at 37 °C for 30 min. Electron spin resonance spectra were recorded using a Bruker EMX spectrometer at 9.78 GHz, 20 mW with a modulation amplitude of 1.0 G, and quantified by adding the total height of eight peaks relative to baseline.

Superoxide measurement by lucigenin.

Lucigenin luminescence measurements were carried out using 30 μM lucigenin[29]. When added, p47*phox*, p67*phox* and Rac1(GTP-γS) were at 1 μM.

Soft agar assay.

Trypsinized cells were suspended in medium containing DMEM, 10% fetal bovine serum, 100 units ml^{-1} penicillin, 100 μg ml^{-1} streptomycin and 0.3% noble agar (Difco, Detroit) with or without puromycin; 1.5×10^5 cells per well were plated in six-well plates onto solidified medium containing 1% noble agar. Plates were incubated at 37 °C in 5% CO_2, and medium was added every 5–7 days. After 19 days, cells were incubated overnight with p-iodonitrotetrazolium violet (Sigma) and photographed.

Received 21 May; accepted 16 July 1999.

1. Jones, S. A., Hancock, J., Jones, O. T. G., Neubauer, A. & Topley, N. The expression of NADPH oxidase components in human glomerular mesangial cells: Detection of protein and mRNA for p47*phox*, p67*phox*, and p22*phox*. *J. Am. Soc. Nephrol.* **5,** 1483–1491 (1995).
2. Matsubara, T. & Ziff, M. Increased superoxide anion release from human endothelial cells in response to cytokines. *J. Immunol.* **137,** 3295–3298 (1986).
3. Meier, B. *et al.* Human fibroblasts release reactive oxygen species in response to interleukin-1 or tumor necrosis factor-α. *Biochem. J.* **263,** 539–545 (1989).
4. Pagano, P. *et al.* Localization of a constitutively active, phagocyte-like NADPH oxidase in rabbit aortic adventitia: Enhancement by angiotensin II. *Proc. Natl Acad. Sci. USA* **94,** 14483–14488 (1997).
5. Jones, S. *et al.* Expression of phagocyte NADPH oxidase components in human endothelial cells. *Am. J. Physiol.* **271,** H1626 (1996).
6. Griendling, K. K., Minieri, C. A., Ollerenshaw, J. D. & Alexander, R. W. Angiotensin II stimulates NADH and NADPH oxidase activity in cultured vascular smooth muscle cells. *Circ. Res.* **74,** 1141–1148 (1994).
7. Szatrowski, T. P. & Nathan, C. F. Production of large amounts of hydrogen peroxide by human tumor cells. *Cancer Res.* **51,** 794–798 (1991).
8. Burdon, R. Superoxide and hydrogen peroxide in relation to mammalian cell proliferation. *Free Rad. Biol. Med.* **18,** 775–794 (1995).
9. Crawford, D., Zbinden, I., Amstad, P. & Cerutti, P. Oxidant stress induces the proto-oncogenes c-*fos* and c-*myc* in mouse epidermal cells. *Oncogene* **3,** 27–32 (1988).
10. Nose, K. *et al.* Transcriptional activation of early-response genes by hydrogen peroxide in a mouse osteoblastic cell line. *Eur. J. Biochem.* **201,** 99–106 (1991).
11. Datta, R. *et al.* Involvement of reactive oxygen intermediates in the induction of c-jun gene transcription by ionizing radiation. *Biochemistry* **31,** 8300–8306 (1992).
12. Bae, Y. S. *et al.* Epidermal growth factor (EGF)-induced generation of hydrogen peroxide. *J. Biol. Chem.* **272,** 217–221 (1997).
13. Zafari, A. M. *et al.* Role of NADH/NADPH oxidase-derived H_2O_2 in angiotensin II-induced vascular hypertrophy. *Hypertension* **32,** 488–495 (1998).
14. Wolin, M. S. Activated oxygen metabolites as regulators of vascular tone. *Klin. Wochenschr.* **69,** 1046–1049 (1991).
15. Sundaresan, M., Zu-Xi, Y., Ferrans, V. J., Irani, K. & Finkel, T. Requirement for generation of H_2O_2 for platelet-derived growth factor signal transduction. *Science* **270,** 296–299 (1995).
16. Irani, K. *et al.* Mitogenic signaling mediated by oxidants in Ras-transformed fibroblasts. *Science* **275,** 1649–1652 (1997).
17. Segal, A. W. & Shatwell, K. P. The NADPH oxidase of phagocytic leukocytes. *Ann. NY Acad. Sci.* **832,** 215–222 (1997).
18. Royer-Pokora, B. *et al.* Cloning the gene for an inherited human disorder–chronic granulomatous disease–on the basis of its chromosomal location. *Nature* **322,** 32–38 (1986).
19. Wallach, T. M. & Segal, A. W. Analysis of glycosylation sites on gp91phox, the flavocytochrome of the NADPH oxidase, by site-directed mutagenesis and translation in vitro. *Biochem. J.* **321,** 583–3746 (1998).
20. Bjorgvinsdottir, H. Zhen, L. & Dinauer, M. Cloning of murine gp91phox cDNA and functional expression in a human X-linked chronic granulomatous disease cell line. *Blood* **87,** 2005–2010 (1996).
21. Rotrosen, D. Yeung, C. L., Leto, T. L. & Malech, K. C. H. Cytochrome b_{558}: The flavin-binding component of the phagocyte NADPH oxidase. *Science* **256,** 1459–1462 (1992).
22. Segal, A. W. *et al.* Cytochrome b_{-245} is a flavocytochrome containing FAD and the NADPH-binding site of the microbicidal oxidase of phagocytes. *Biochem. J.* **284,** 781–788 (1992).
23. Sumimoto, H. *et al.* Cytochrome b_{558}, a component of the phagocyte NADPH oxidase, is a flavoprotein. *Biochem. Biophys. Res. Commun.* **186,** 1368–1363 (1992).
24. Berk, B. C., Elder, E. & Mitsuka, M. Hypertrophy and hyperplasia cause differing effects on vascular smooth muscle cell Na^+/H^+ exchange and intracellular pH. *J. Biol. Chem.* **265,** 19632–19637 (1990).
25. Gardner, P., Raineri, I., Epstein, L. & White, C. Superoxide radical and iron modulate aconitase activity in mammalian cells. *J. Biol. Chem.* **270,** 13399–13405 (1995).
26. Fridovich, I. Superoxide anion radical (O_2^-), superoxide dismutases, and related matters. *J. Biol. Chem.* **272,** 18515–18517 (1997).
27. Gardner, P. R., Znguyen, D. H. & White, C. W. Aconitase is a sensitive and critical target of oxygen poisoning in cultured mammalian cells and in rat lungs. *Proc. Natl Acad. Sci. USA* **91,** 12248–12252 (1994).
28. Flint, D. H. Initial kinetic and mechanistic characterization of *Escherichia coli* fumarase A. *Arch. Biochem. Biophys.* **311,** 509–513 (1994).
29. Li, Y. *et al.* Validation of lucigenin (bis-*N*-methylacridinium) as a chemiluigenic probe for detecting superoxide anion radical production by enzymatic and cellular systems. *J. Biol. Chem.* **273,** 2015–2023 (1998).

Acknowledgements

We thank D. Jones and D. Edmondson for discussions and technical advice; W. Sun for technical assistance; and D. Dillehay for the histological analysis. This work was supported by the NIH.

Correspondence and requests for materials should be addressed to J.D.L. (e-mail: dlambe@bimcore.emory.edu).

NF-κB activation by tumour necrosis factor requires the Akt serine–threonine kinase

Osman Nidai Ozes*, Lindsey D. Mayo*, Jason A. Gustin*, Susan R. Pfeffer†, Lawrence M. Pfeffer† & David B. Donner*

** Department of Microbiology and Immunology, Indiana University School of Medicine and the Walther Oncology Center, Indianapolis, Indiana 46202, USA*
† Department of Pathology, University of Tennessee Health Science Center, Memphis, Tennessee 38163, USA

Activation of the nuclear transcription factor NF-κB by inflammatory cytokines requires the successive action of NF-κB-inducing kinase (NIK) and an IκB-kinase (IKK) complex composed of IKKα and IKKβ[1–5]. Here we show that the Akt serine–threonine kinase[6] is involved in the activation of NF-κB by tumour necrosis factor (TNF). TNF activates phosphatidylinositol-3-OH kinase (PI(3)K) and its downstream target Akt (protein kinase B). Wortmannin (a PI(3)K inhibitor), dominant-negative PI(3)K or kinase-dead Akt inhibits TNF-mediated NF-κB activation. Constitutively active Akt induces NF-κB activity and this effect is blocked by dominant-negative NIK. Conversely, NIK activates NF-κB and this is blocked by kinase-dead Akt. Thus, both Akt and NIK are necessary for TNF activation of NF-κB. Akt mediates IKKα phosphorylation at threonine 23. Mutation of this amino acid blocks phosphorylation by Akt or TNF and activation of NF-κB. These findings indicate that Akt is part of a signalling pathway that is necessary for inducing key immune and inflammatory responses.

NF-κB regulates gene expression in immunity, stress responses, inflammation[7] and the inhibition of apoptosis[8,9]. Ordinarily, NF-κB is sequestered in the cytoplasm by the inhibitory protein IκB. Ultraviolet radiation, T-cell activation, bacterial lipopolysaccharide, viral gene products and inflammatory cytokines promote IκB degradation, thereby allowing NF-κB to enter the nucleus and induce gene transcription[7]. Activation of the type-1 TNF receptor